Vortex pinning in the frozen vortex lattice in $YBa_2Cu_3O_{7-x}$ films

Dimitrios G. Xenikos,* Anne E. Cunningham, and Thomas R. Lemberger
Department of Physics, Ohio State University, Columbus, Ohio 43210

L. Hou and Michael McElfresh
Department of Physics, Purdue University, West Lafayette, Indiana 47907

(Received 12 June 1995; revised date received 10 November 1995)

The inductance of vortices $L_V(T,B)$ in $YBa_2Cu_3O_{7-x}$ films is studied for temperature $8<T<85$ K, and magnetic field $0<B<6$ T with the goal of identifying the morphology of the vortex pinning sites and the type of the glass phase below the vortex lattice melting transition $B_g(T)$. The key feature that distinguishes point, linear, and planar pinning sites is how rapidly L_V increases when thresholds in T and B are crossed. We find that, below a threshold field $B_p(T)<B_g(T)$, the effective pinning force on each vortex is independent of B. At $B_p<B<B_g$, L_V increases as B^2, whereas at $B\approx B_g$, L_V diverges faster than B^2 following a scaling law on f, consistent with a phase transition between a glass and a liquid vortex state. Although the value of the threshold field, $B_p\approx 8(1-T/T_C)$ T, is consistent with any type of pinning defect, the increase of $L_V\propto B^2$ for $B>B_p$ is much less rapid than predicted for collective pinning of vortices by point defects. Linear and planar defects are possible explanations, but the necessary theoretical calculations are currently absent.

I. INTRODUCTION

While it is well known that some sort of defect in $YBa_2Cu_3O_{7-x}$ (YBCO) films pins vortices very effectively, the identity of the defect is as yet undetermined. Candidate defects include oxygen and other vacancies, dislocations perpendicular to the film, and twin planes. All of these defects exist in films, so the actual situation is rather complicated. Theoretical work is extensive along mainly two directions: First, the collective pinning model considers vortex pinning on pointlike disorder and predicts a ''vortex-glass'' low-temperature state that melts at a phase boundary $B_g(T)$.[1] Second, the ''Bose-glass'' model studies vortex pinning on line defects and finds a qualitatively different glass state and phase boundary.[2,3] Most of the time, theory focuses on prototypical materials containing one type of defect, and is generally successful in case where these materials can be generated experimentally, as with columnar defects generated by heavy-ion irradiation of an initially weakly pinning YBCO crystal[4] and by studies of clean YBCO crystals before and after twin planes have been removed.[5] These simplified theoretical models can be brought to bear on films when one measures a parameter which behaves very differently for different morphologies of pinning sites. Such a parameter is the inductance $L_V(T,B)$ of pinned vortices, which is inversely proportional to the effective pinning force constant.

This paper reports an experimental study of the inductance of vortices in a long, narrow film of YBCO in the region of temperatures, fields, and frequencies where the vortex lattice is ''frozen,'' vortices are fully pinned and therefore inductive, and the inductance is a direct probe of the pinning strength. In this region of the phase space, which lies below the phase boundary $B_g(T_g)$ between glass and liquid vortex phases, L_V is inversely proportional to the effective vortex pinning force constant α_L, referred to as the Labusch parameter. L_V is conventionally reduced to the Campbell penetration depth squared $\lambda_C^2(T,B)\propto L_V\propto 1/\alpha_L$, where the proportionality constants involve geometric factors and universal constants. The usefulness of this convention is that it facilitates comparison of the vortex inductance to the kinetic inductance of the superconducting electrons, which is proportional to the *ab*-plane penetration depth, λ^2. Qualitative expectations of any model are that, as T or B increases, pinning of the vortex lattice softens so that λ_C^2 increases until it diverges at the melting curve $B_g(T)$. One point of deviation between theoretical models is the magnitude of the pinning force constant at low temperatures in the glass phase, which may distinguish regions of phase space where vortices are pinned individually or collectively. A second important difference between models lies in how rapidly pinning decreases as T and B increase beyond important thresholds. The key idea is that pinning by point defects is marginal and easily disrupted by thermal fluctuations and intervortex repulsion, whereas pinning by linear and planar defects are much more robust and could lead to a milder dependence of λ_C^2 on T or B. At present, explicit expressions for λ_C^2 exist only for collective pinning model for point defects.[11] However, examination of expressions for the effective potential for the line and planar defect models reveals how robust pinning is in these cases.

Experimental study of the inductance of the frozen vortex lattice in films is just beginning. Much more attention has been paid to complex impedance measurements near and above the transition at $B_g(T)$ for comparison of its scaling characteristics to those of the low-frequency nonlinear resistivity.[6–8] Recent experimental studies at microwave frequencies have explored the vortex surface impedance at regions that partially overlap the range $8\leq T\leq 85$ K and $0\leq B\leq 6$ T of our experiment, and estimated the vortex pinning force constant.[9,10] Apart from the extended temperature and field range, our work provides a quantitative comparison of the Campbell penetration length λ_C and the magnetic penetration depth λ in the film, which facilitates the test of theoretical predictions for a variety of types of pinning defects.

 © 1996 The American Physical Society

To gain some insight into how different types of disorder translate into very different dependencies of λ_C on T and B, we consider the collective pinning model by point defects. Within various approximations, Koshelev and Vinokur[11] (KV) have estimated the dependence of λ_C (or L_V) on T and B in the vortex solid phase, focusing on the lattice softening that precedes the melting transition. Pinning is marginal in the following sense. If vortices were rigid rods, then each would intersect about the same number of pinning centers as it passed through the sample, regardless of its location. Hence, no position would be favored over any other position, and pinning would vanish. Random spatial fluctuations in the density of point defects, combined with a flexible vortex line enable individual vortices to curve through the sample in a way that maximizes the number of intersecting pinning sites at the minimum cost in the vortex line energy. Pinning is strongest at low temperatures where thermal fluctuations are small and at low fields where intervortex repulsion is small. Thermal fluctuations reduce pinning very abruptly when thermal motion of each vortex exceeds the range of the pinning potential. Similarly, intervotex repulsion reduces pinning very abruptly when it exceeds a certain threshold and forces vortices to be parallel to each other. The KV theory predicts $\lambda_C \approx \lambda \exp(T^3/T_{p0}^3)$ above a crossover temperature T_{p0} and at low B. It also predicts $\lambda_C \approx \lambda \exp[(B/B_p)^{3/2}]$ above a crossover field B_p. The data show milder increases with T and B and suggest that the vortex pinning sites are extended rather than pointlike.

While it may seem obvious that vortex pinning would decrease monotonically with T and B, this result is not trivial. Feigel'man and Vinokur[12] find theoretically that the critical current density J_c which depins the vortices can increase with increasing B under some circumstances, implying stronger pinning and therefore a decrease in L_V (or λ_C), which is not observed in our films. It would be very interesting to observe simultaneous increases in J_c and L_V.

II. EXPERIMENTAL METHOD AND MODELING

This paper examines the inductance $L_b(B,T)$ of superconducting films, patterned into a long narrow bridge, in the presence of a magnetic field parallel to the *c*-crystallographic axis, using a small ac probe current. This technique has been used in studies of the pinning force constant in YBCO films away from the melting transition at only a few temperature values,[13] and with emphasis on vortex pinning when the field is perpendicular to the *c* axis.[14]

The epitaxial film in our work was deposited by laser ablation on a heated $SrTiO_3$ substrate. The film was 2500 $\pm$400 Å thick, with its *c* axis perpendicular to the film plane and exhibited a sharp transition (the 20%–80% transition width was less than 2 K). From two-coil mutual inductance measurements before the film was patterned we found that the penetration depth fits $\lambda = \lambda_0[1-(T/T_C)^2]^{-1/2}$, with $\lambda_0 = 1730 \pm 400$ Å, to the accuracy demanded by our experiment.[15] The film was patterned into a four-contact microbridge of width 35 μm and length 600 μm between the center lines of the two voltage leads by usual photolithographic techniques and wet etching in dilute nitric acid. The voltage leads were also 35 μm wide, each. As is shown schematically in Fig. 1, the transport current turns antiparallel

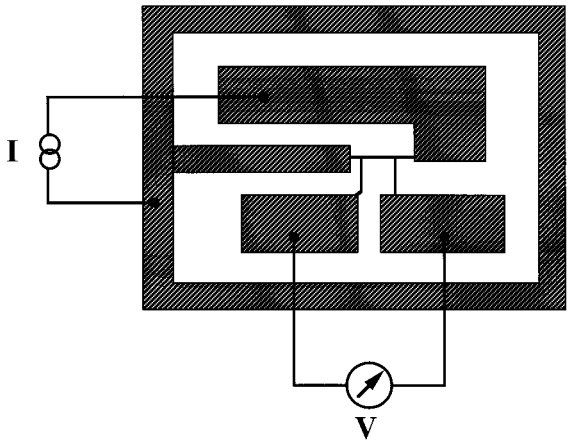

FIG. 1. The geometry used in our experiment.

relative to its direction between the voltage contacts to minimize the induced magnetic field away from the microstrip. The contacts were defined by ion milling (to clean the film surface) and subsequent Ag deposition (0.5 μm thick). The zero-resistance temperature of the film at $B=0$ was 88.5 K.

Measurements were taken in the transport bridge by using a square pulse current of frequency 10^2–2×10^7 Hz and a lock-in amplifier to measure the amplitude and the phase of the signal from the sample. The current was kept small compared with the critical current of the bridge, so that the measured ac voltage V was linear in I at all temperatures of interest. For $0.05<f<20$ MHz, it was necessary to heterodyne the sample response into an audio frequency signal detectable by the lock-in. Special care was taken to eliminate reflections in the transport lines from load mismatch by inserting 50Ω resistors in series with the sample (which is essentially a short, as its complex impedance never exceeds 10 mΩ in our measurements). We used excitation currents as low as 30 μA to ensure that the bridge impedance is purely inductive (i.e., the voltage is 90° ahead of the current within our resolution), at temperatures $T \ll T_c$ and $B=0$. The heat leak from the wires meant that the probe operated at 8 K with helium gas in the sample chamber and above 50 K when evacuated.

Typical data of the inductance of our microbridge at $f=2$ MHz are plotted in Fig. 2. In this plot, one observes the increase of the inductance with the application of a magnetic field $B=1$ T relative to the zero-field data. Deducing the inductance of the vortices from such set of inductance data is not as simple as subtracting the zero-field from the in-field data at the same temperature, because the distribution of supercurrent across the film width changes with magnetic field. We should, therefore, construct an appropriate model that incorporates the fact. Similar concepts are involved in modeling the microstrip resonator measurements in Ref. 10. In the remainder of this section, we calculate the measured ac voltage V in a typical four-terminal microbridge, identify its terms that depend on temperature and magnetic field.

L_b comprises three contributions ($L_b = L_p + L_k + L_v$), all of which depend on the bridge length s, width w, and thickness d. The largest, L_p, is the contribution from the magnetic flux through a closed path that includes the center line of the

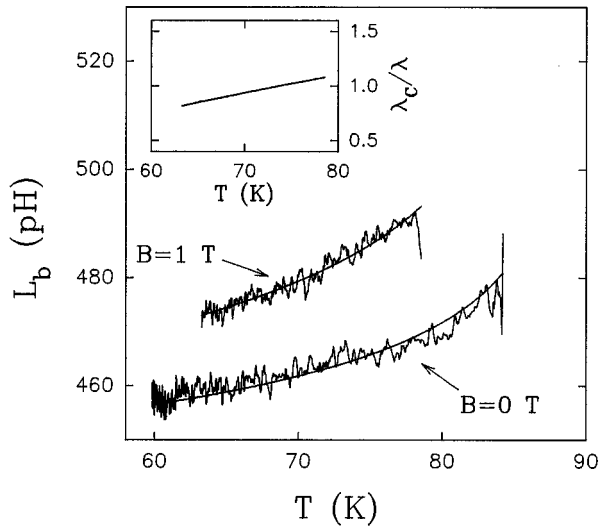

FIG. 2. Temperature dependence of the inductance of the microbridge at $B=0$ and $B=1$ T, for $f=2$ MHz. Inset: The ratio λ_C/λ determined from these data using the model Eq. (6).

microstrip and the wires to the lock-in, generated in the voltage loop by the drive current in the microstrip. By approximating the film as a long wire of radius $w/2$ and taking the voltage pickup loop to be rectangular $s\times r$ ($r\approx 3$ mm), there results

$$L_p\approx\mu_0 s[1+2\ln(2r/w)]/4\pi\approx 11.3\mu_0 s/4\pi\approx 680 \text{ pH}.$$

A numerical calculation for a long thin film rather than a long cylindrical wire increases this number by 10%. Since the actual bridge is not much longer than the spacing between the voltage electrodes, this number overestimates the actual coupling from currents in the bridge itself. It is essential to remember that within the bridge, the supercurrent density J_s peaks at the film edges to a degree determined by the ratio $Y^2\equiv wd/\lambda_{\rm eff}^2$, where $\lambda_{\rm eff}(T,B)$ is an effective *ab*-penetration depth defined in detail below and which, at $B=0$, equals $\lambda(T)$. This is a well-known solution of Maxwell's equations coupled with London's equation for transport current in the strip geometry, for the strict limit $\lambda_{\rm eff}\gg d$. Pyun *et al.*[16] have tested the theoretical prediction for J_s by measuring nonuniform supercurrent densities in a low-T_C superconductor, and verified that the model holds for more realistic microstrips with values of Y up to about 5. From their work, we conclude that a nonuniform J_s results in an inductance L_p well approximated by

$$L_p(Y)\approx L_{p0}(1-\beta_1 Y) \tag{1}$$

with $\beta_1=0.014$ for values $1<Y<19$ encountered in this work. This equation captures the dependence of L_p on temperature and magnetic field, since the effect of vortices is to increase $\lambda_{\rm eff}$.

Another contribution to L_b is the zero-magnetic-field kinetic inductance L_k, which arises from the electric field accelerating the superconducting electrons. If J_s were uniform, then $L_k=\mu_0\lambda^2 s/wd$, representing around 1% of the L_p estimated above. Taking into account the nonuniform J_S, and using the same integration loop as in the calculation in Eq. (1) that includes the centerline of the microbridge, we find

$$L_k\approx\mu_0 s(1-\beta_2 Y)/(wd/\lambda^2) \tag{2}$$

with $\beta_2=0.051$ for the values of Y encountered here. The fact that this formula allows a negative L_k indicates the breakdown of the simple approximation of the dependence of L_k on Y at large Y. For our experiment, the important physics is that L_k increases monotonically with decreasing Y, and Eq. (2) expresses this.

The third contribution to L_b is the additional kinetic inductance L_v from the vortices. L_v is most easily discussed in the context of a single pinned vortex. The applied supercurrent produces a force $\phi_0 J_s$ per unit length on the vortex, in a direction perpendicular to the supercurrent. This force is matched by the pinning force per unit length αx, plus a viscous force ηv_x, where x is the displacement of the vortex from the center of the pinning potential which is assumed quadratic with curvature α. The average value of α is designated the Labusch parameter α_L. Solving for the velocity of the vortex motion v_x, we calculate the amplitude of the voltage generated on the bridge in the presence of applied magnetic field

$$V=(B\phi_0/\eta)(I_{\rm ac}s/wd)[-i\omega/(-i\omega+\alpha/\eta)], \tag{3}$$

with $I_{\rm ac}$ the amplitude of the current through the strip.

If there is no pinning, as in temperatures close to the T_C, then $\alpha=0$, and $V=(B\phi_0/\eta)(s/wd)I_{\rm ac}$ is in phase with the current. The Bardeen-Stephen model for free flux flow, and the measurements in YBCO films of Kunchur *et al.*[17] at temperatures close to the T_C, suggest that $\eta=B_{c2}\phi_0/\rho_n$, with characteristic values for the upper critical field $B_{c2}(T)\approx 2(T_C-T)$ in units *T/K*, and normal state resistivity $\rho_n(T)\approx 70(T/100)$, in $\mu\Omega$ cm. At much lower temperatures, where the vortices are pinned ($\alpha>0$) and the frequency of the current is low ($\omega\ll\alpha/\eta$), the viscous force is negligible, and the impedance of the vortices is inductive. Physically, this inductance represents a net reduction in the average superfluid density due to the supercurrents around the moving vortices. As with L_k, L_V should reflect the reduced current density along the centerline of the film. The inductance L_V from the vortex motion is therefore

$$L_V=(B\phi_0/\alpha_L)(s/wd)(1-\beta_2 Y)\equiv\mu_0\lambda_C^2(s/wd)(1-\beta_2 Y), \tag{4}$$

where we used the conventional definition of the Campbell length, λ_C. As $B\to 0$, the Campbell length λ_C vanishes.

It remains to define $\lambda_{\rm eff}$. The fact that the distribution of supercurrent in the film is determined by the sheet inductance suggests that $\lambda_{\rm eff}^2=\lambda^2(T)+\lambda_C^2(T,B)$. However, even if the vortices were immobile ($\alpha_L\to\infty$ and $\lambda_C^2\to 0$), the applied field would reduce the superfluid density by a factor $[1-B/B_{c2}(T)]$. We choose the simplest field dependence of$\lambda_{\rm eff}$ and write

$$\lambda_{\rm eff}^2=[\lambda^2(T)+\lambda_C^2(T,B)]/[1-B/B_{c2}(T)]. \tag{5}$$

This expression is in agreement with the electrodynamics model of Clem and Coffey.[18] In fact though, in the T and B range in our experiment, the field term in Eq. (5) plays a minor role.

To summarize, the bridge inductance is a function of T and B through its dependence on $\lambda_{\rm eff}$, as parametrized by $Y^2 \equiv wd/\lambda_{\rm eff}^2$, through the model equation

$$L_b = L_{p0}[1-\beta_1 Y] + \mu_0 s[1-\beta_2 Y]/Y^2. \qquad (6)$$

This is the fundamental equation of our model that includes the corrections from the nonuniform current distribution. It enables the deduction of $\lambda_C(T,B)$ from $L_b(T,B)$. For a long narrow strip, where the supercurrent distribution is close to that in an infinitely long bridge, Pyun *et al.*[16] estimate $\beta_1 = 0.014$ and $\beta_2 = 0.051$. In the pattern used in our experiment (Fig. 1), where the current runs antiparallel to the bridge to minimize L_{p0}, we estimate from geometrical considerations $L_{p0} \approx 500$ pH, $\beta_1 = 0.005$ and $\beta_2 = 0$. The actual value of these parameters will be determined from best fits to our data. Since our results agree with results of quite different techniques at low B and T, we are confident that this model is sufficiently accurate for our purposes.

Actually, the main conclusions of this paper would be the same, qualitatively, even if we took J_s to be the uniform. However, for a quantitative determination of $\lambda_C(T,B)$, the assumption of a uniform J_S is valid *only very close to* T_g. In that restricted T and B region, $\lambda_C/\lambda \to \infty$ and $Y^2 \to 0$, so the term $L_{p0}[1-\beta_1 Y] + \mu_0 s \beta_2 / Y$ can be treated as a quantity independent of B and T, compared to the quadratic term $\mu_0 s/Y(T,B)^2$ that changes much faster. Then, λ_C^2 is estimated by subtracting the zero-field data from the field data, similarly as if J_S were uniform:

$$L_b(T,B) - L_b(T,B=0) \approx \mu_0 \lambda_C(T,B)^2 s/(wd), \qquad (7)$$

$$\text{when } \lambda_C(T,B)/\lambda(T) \to \infty.$$

This is an important limit of Eq. (6), especially for frequency-dependent studies close to T_g (Refs. 6–8). There, a small f dependence in L_{p0}, that typically arises due to limitations of the experimental setup, is negligible compared to the strong dependence of Y^2 on B, T, and f. However, in the present work we focus on the dynamics of the frozen vortex lattice at $T < T_g$, thus our analysis is based on Eq. (6), where we take into account the nonuniform current distribution in the bridge.

III. EXPERIMENTAL RESULTS

We begin analysis of the temperature-dependence data at $f = 2$ MHz (Fig. 2) by looking at those for $B = 0$, where no vortices are present and λ_C should vanish. The very good fit shown by the smooth curve in the figure is obtained using Eq. (6) with $L_{p0} = 480$ pH, $\beta_1 = 0.004$ and $\beta_2 = 0.015$ very close to their expected values. [Equally excellent fits can be obtained with $480 < L_{p0} < 520$ pH, $0.0035 < \beta_1 < 0.006$ and $0 < \beta_2 < 0.030$, even if we vary $\lambda(T=0)$ between 1730 and 2400 Å to bracket plausible values. In the fitting procedure, the curvature of the $L_b(B=0,T)$ data obliges a nonzero β_1, and confirms our concern about the effect of a nonuniform current distribution in the film.] Then, by using Eq. (6) with the same parameter values for the data at $B = 1$ T, we determine the λ_C/λ shown in the graph inset. We should emphasize that the value of λ_C/λ as well as its modest temperature dependence (by ~10%) at $B = 1$ T are *not* sensitive to the particular values of L_{p0}, β_1, or β_2 chosen for the fit. This is also true for our B dependence data that we analyze below.

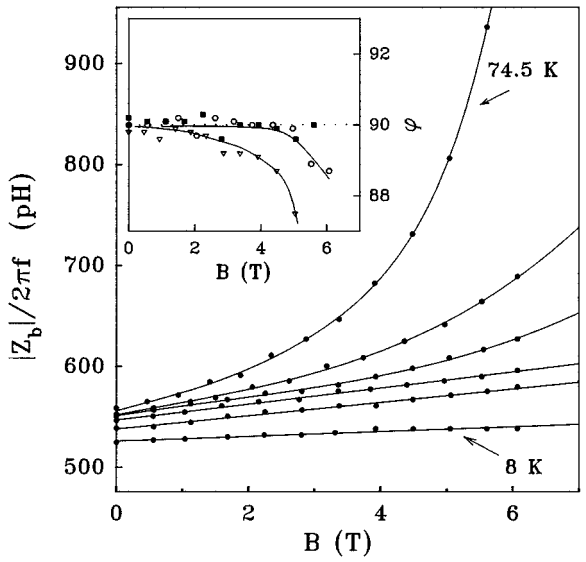

FIG. 3. Magnitude $|Z_b| 2\pi f$ of the impedance for $T = 8$, 54.1, 60.0, 65.5, 70.0, and 74.5 K. Inset: phase ϕ of the impedance at $T = 65.5$ K (circles), 70.0 K (squares), and 74.5 K (triangles). At $T = 74.5$ K and $B > 4$ T, ϕ drops below 90°, indicating a small resistive component to Z_b, as B approaches the melting field

In Fig. 3 we show the field dependence of the magnitude $|Z_b|/2\pi f$ and the phase ϕ of the bridge impedance at $f = 1$ MHz. Since ϕ is always very close to 90°, $|Z_b|/2\pi f \equiv L_b$ is essentially inductive. As in Fig. 1, the data were taken at $I_{\rm ac}/dw = 600$ A/cm^2, i.e., as much as 3 orders of magnitude smaller than the critical current density. There are several features to note. First, at $B = 0$ where there are no vortices, $L_b(T,B=0)$ increases with T, as is expected from the increase in the intrinsic penetration depth and Eq. (2). Second, at fixed T, L_b increases linearly with B, i.e., proportional to the density of vortices, below a threshold field $B_p(T)$. $B_p(T)$ increases from something greater than 6 T at 8 K to about 1 T at 74.5 K, and the slope, $\partial L_b/\partial B|_T$, increases. These features of the data are reflected, through Eq. (6), to the quantity *T(T,B)* (plotted in Fig. 4), and finally to the ratio λ_C/λ (plotted in Figs. 5 and 6). The fit parameters used are $L_{p0} = 569$pH, $\beta_1 = 0.004$, and $\beta_2 = 0.015$. The 15% difference of L_{p0} compared the value 480 pH for the 2 MHz data of Fig. 2, is indicative of a small variation of the impedance data at frequencies $f \geq 2$ MHz, which results from unavoidable nonperfect termination of the 50 Ω transport lines, and is very reproducible on a day-to-day basis.

The field $B_p(T)$ marks a crossover between qualitatively different responses of the vortex system to the small perturbations induced by the excitation current in our film bridge. Although this crossover can be seen in the raw data (Fig. 3), we define $B_p(T)$ from Fig. 5, where the data are corrected for the nonuniform current distribution in the strip. This operational definition does not alter qualitatively our conclusions, but is more appropriate for comparison of the measured $B_p(T)$ with theoretical predictions. As shown in Fig. 5, $(\lambda_C/\lambda)^2$ approaches zero with a nonzero slope for

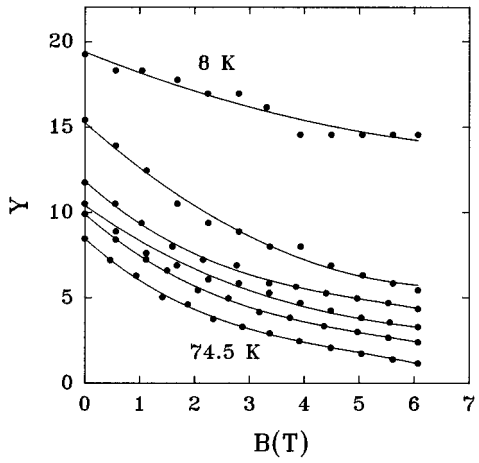

FIG. 4. Values of *Y(B,T)* extracted from the data of Fig. 3, using our model Eq. (6). The lines are guides to the eye.

$B<B_p(T)$, which indicates that in this region of phase space the vortex pinning force $\alpha_L \equiv \phi_0 B/\mu_0 \lambda_C^2$ is independent of the magnetic field. On the other hand, at $B>B_p(T)$, $(\lambda_C/\lambda)^2$ increases as B^2, as shown in Fig. 6, over a wide range of fields and temperatures. Thus, for $B>B_p(T)$ $\alpha_L \propto 1/B$, indicating that the pinning strength is inversely proportional to the density of vortices. Collecting the values of $B_p(T)$ from our experimental data, we note two phenomenological characteristics: First, its temperature dependence is consistent with the form $B_p=(8\ \mathrm{T})[1-T/T_C]$ (shown in the inset of Fig. 7). Second, as indicated in Fig. 6,

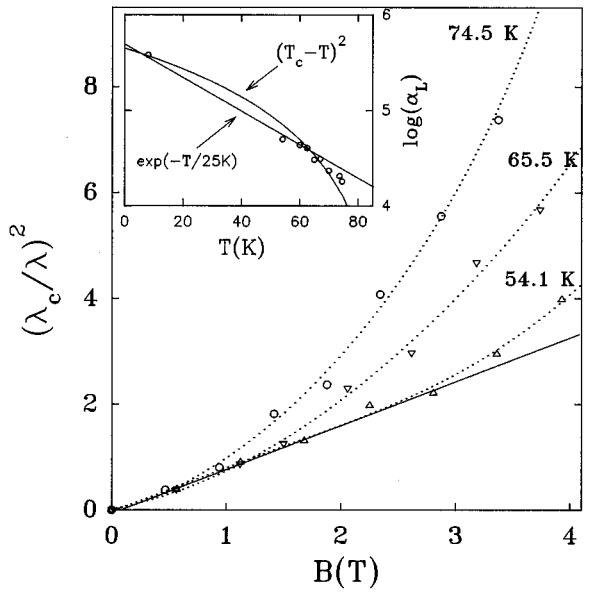

FIG. 5. Typical curves $(\lambda_C/\lambda)^2$ vs B, for $\lambda(T)^2=(1730\ \text{Å})^2/(1-T^2/T_C^2)$. The data approach the origin with a nonzero slope (as indicated by the solid line for the case of 54.1 K) and they diverge above a crossover field $B_p(T)$. Inset: Labush parameter $a_L(T)$ in units N/m^2 (expressed in logarithm base 10) for $B<B_p$. The line $\alpha_L \propto \exp(-T/25\ \mathrm{K})$ describes phenomenologically the experimental results of Golosovski *et al.* (Ref. 9), taken on similar films with a different technique. The curve $\alpha_L \propto (T_c-T)^2$ is the theoretical prediction of the Bose-glass model (Ref. 2). Both curves are consistent with our data.

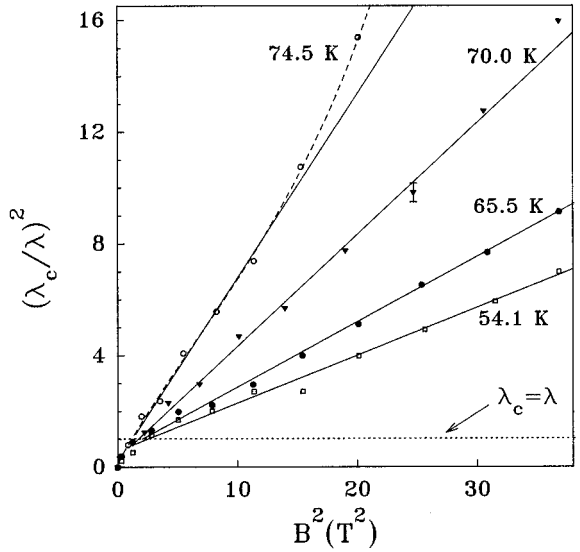

FIG. 6. The ratio $(\lambda_C/\lambda)^2$ plotted vs B^2 for T=54.1, 65.5, 70.0, and 74.5 K. The solid lines indicate $(\lambda_C/\lambda)^2 \propto B^2$ when $\lambda_C>\lambda$. The dashed line through the data at 74.5 K indicates a faster than B^2 increase of $(\lambda_C/\lambda)^2$ upon approaching the melting field $B_g=5.4\pm0.4$ T.

B_p marks the deviation of λ_C/λ from, roughly, unity. The importance of these two features will be discussed extensively in the following section.

For completeness, we also measure the frequency dependence of the bridge inductance. This is important since, in the vicinity of a phase line $B_g(T_g)$, the inductive vortex response has been shown to follow a power law, $L_V \propto f^{-\zeta}$ ($\zeta>0$), consistent with a phase transition at $B_g(T_g)$ separating a glass from a liquid vortex state.[19] This signifies a *frequency-dependent* increase of L_V when approaching T_g, which should be distinguished from the B^2 increase of the $(\lambda_C/\lambda)^2$ that we observe. Therefore, in Fig. 7 we plot the exponent $\zeta(T)$ for our highest magnetic field value (B=6 T) from data taken at frequencies $0.05<f<20$ MHz. The error bars represent the uncertainty in ζ due to a $\pm10\%$ fluctuation

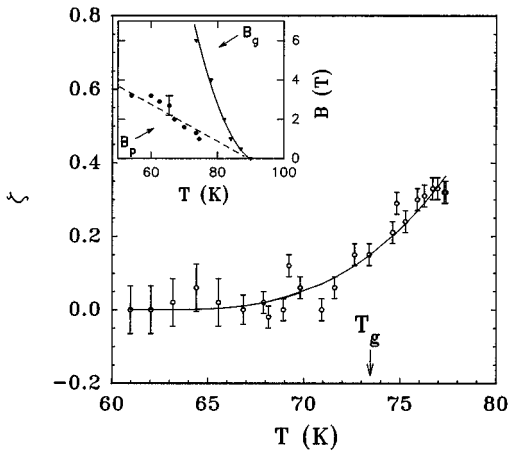

FIG. 7. Frequency dependence of the scaling exponent $\zeta(T)$ at B=6 T. The smooth line through the data is a guide to the eye, and the arrow indicates the melting temperature T_g. Inset: phase diagram with $B_g(T)$ and $B_p(T)$ lines.

of L_{p0} as a function of frequency. We see that $\zeta(T)$ deviates from zero only a couple of degrees below $T_g(B=6T) = 73.7 \pm 0.7$ K, which is determined from nonlinear resistivity *I-V* curves at 100 Hz following conventional procedures.[20,21] That leaves a large portion of phase space between the phase lines $B_p(T)$ and $B_g(T)$ (inset of Fig. 7) where $(\lambda_C/\lambda)^2 \propto B^2$ *and* frequency independent, a range which we examine in this report. Details on the frequency-dependent complex impedance and on the nonlinear low-frequency conductivity in the vicinity of the B_g, as well as the determination of the critical exponents and the magnitude of the correlation length and time of the transition are published separately.[8]

IV. DISCUSSION

It is useful, at first, to extract some numbers from the low-temperature α_L data, shown in Fig. 5 (inset). An estimate for the maximum α_L comes from equating the pinning energy per unit length, $H_c^2 \pi \chi_{ab}^2/2\mu_0$, for a cylindrical hole of radius ξ_{ab} to the depth of the pinning well, $U_p = \alpha_L \xi_{ab}^2/2$. Then, $\alpha_L = H_c^2 \pi/\mu_0$. With $H_c \approx 1.2$ T at $T=8$ K, this yields to $\alpha_L^{\max} \approx 3.6 \times 10^6$ N/m^2, which is a decade stronger than the observed, and apparently leaves some room for improvement of the vortex pinning in films. Furthermore, α_L can be converted to a critical current density j_{c0} by equating the Lorenz force per unit length, $j_{c0}\phi_0$, to the maximum pinning force per unit length, $\alpha_L \xi_{ab}$, assuming that the range of the pinning potential is roughly equal to the *ab*-plane coherence length $\xi_{ab} \approx 14$ Å. With $\alpha_L = 6 \times 10^5$ N/m^2, this yields to $j_{c0} = 42$ MA/cm^2, which is reasonable for a good film. Thus, the low-temperature data are quite reasonable and they argue that the model is correct and the film is of good quality.

The observed temperature dependence of the Labusch parameter indicates that the vortices *are not* independently pinned in the defect structure of the films. The pinning energy per unit length for a vortex core, sitting on a cylindrical defect of radius defect ξ_{ab}, is $H_c^2 \pi \xi_{ab}^2/2\mu_0 \propto 1/\lambda^2$, which is inconsistent with the decrease (by a factor of 5) of α_L between 8 and 55 K. On the other hand, point defects for vortices singly pinned predict that λ_C is inversely proportional to the critical current in the film, a strong temperature dependence which is not observed. For reference, at $78 < T < 83$ K and $B=1$ T, we measure a change of the critical currents approximately by a factor of 10, to be compared with the modest 10% change of λ_C/λ in the inset of Fig. 2. Furthermore, the fact that α_L is field independent for $B < B_p$ (within our experimental accuracy) means that the average pinning potential acting on each new vortex is the same as that acting on all other vortices. As noted by Revenaz *et al.*,[10] this is inconsistent with the notion of a hierarchy of pinning energies in which each new vortex locates in the strongest available pinning site. It is likely that there is a spread of pinning energies associated with qualitatively different pinning sites, but new vortices distribute themselves in a vortex lattice across all these rather than filling the deepest sites first, so that the average pinning site is independent of *B*.

Models that study how a collection of vortices is pinned on the sample disorder are, thus, appropriate candidates for describing our data. Available models are the collective pinning model for point defects, and the Bose-glass model for pinning on line defects. First, in the collective pinning model for point defects, Koshelev and Vinokur have estimated the dependence of λ_C^2 on T and B in the vortex solid phase, predictions that can be tested directly from our data. From Fig. 5 (inset) we find that the form $\alpha_L \propto \exp(-T/25\ \text{K})$ used in Ref. 9 agrees well with our data. While Golosovski *et al.* took this to be supportive of the applicability of the collective pinning model, we disagree. Since the model expects $\alpha_L \propto \alpha_L(T=0)$ below T_p and $\alpha_L \propto \exp(-T^3/T_p^3)$ above T_p, we conclude that the characteristic temperature T_p would be larger than our highest temperature of 74.5 K in Fig. 3, if the collective pinning model of point defects were to apply on films. This, however, would mean that T_p exceeds (or coincides with) the melting transition $T_g = 73.7 \pm 0.7$ K at $B=6$, while the model expects the exponential behavior to signal the softening of the vortex lattice at temperatures below T_g.

On the other hand, the Bose-glass model of Nelson and Vinokur for pinning in line defects does not calculate $\lambda_C^2(T,B)$ explicitly. However, it predicts that the average vortex pinning energy is $T^* \approx 10(T_C - T) = \alpha_L \chi_{ab}^2$ for $T < 0.95 T_C$. The latter equality assumes that the range of pinning potential is $\sqrt{2}\chi_{ab} \approx \xi_0 (1 - T/T_C)^{-1/2}$. If so, then one finds $\alpha_L = \alpha_L(T=0)(1 - T/T_C)^2$, which is consistent with the data (inset in Fig. 5).

The crossover between the linear and nonlinear behavior of λ_C^2 vs B (inset in Fig. 7) provides another test for the theories. The collective pinning theory predicts at $T < T_p$ that $\lambda_C^2 \propto B$ until λ_C^2 exceeds λ^2 which is not in disagreement with the data. The relation $B_p \approx 8(1 - T/T_C)$ T for $T < 0.9 T_C$ expected in the Bose-glass phase for linear defects spaced by about 200 Å also agrees with the data. The analogous expression for the planar defects is unclear, but it seems likely that all types of pinning centers are consistent with the experimental crossover field.

The most interesting part of this study is the nonlinear behavior of λ_C^2 vs *B*. Experimentally, $(\lambda_C/\lambda)^2 \propto B^2$ in the nonlinear region. This increase falls short of the theoretical expectations for point defects. The KV prediction $\lambda_C(T, B > B_p) \approx \lambda(T) \exp[(B/B_p)^{3/2}]$ expects $\lambda_C^2 \approx 270 \lambda^2$ at 74.5 K and $B=3$ T (taking a conservative value $B_p = 1.5$ T), where we measure only $\lambda_C^2 \approx 4\lambda^2$. Keeping in mind that the KV theoretical expressions quoted do not include higher-order effects that lead to the melting transition, like two-level systems, the discrepancy with the data is even more compelling.

We conclude that the vortex pinning centers are extended rather than pointlike. Unfortunately, we do not have explicit expressions of $\lambda_C(B,T)$ for other types of pinning defects. Since it has been shown from critical current measurements that line defects are more effective pinning centers than point defects, they probably lead to milder increases of λ_C/λ with temperature and field, that could match the behavior observed. Detailed calculations of the inductive response for mesoscopic disorder that incorporate thermal fluctuations are the next step towards understanding the vortex pinning in competing types of disorder, as the ones which exist in thin films.

ACKNOWLEDGMENTS

We kindly acknowledge extended discussions with D. Stroud, M. P. A. Fisher, and S. Hebboul. Support for this work has been provided primarily by AFOSR-91-0188, and also by DOE Grant No. DE-FG02-90ER45427 through MISCON.

*Present address: CNRS-CRTBT, BP 166, 38042 Grenoble cedex 9, France.

[1] G. Blatter, M. V. Feigel'man, V. B. Geshkenbein, A. I. Larkin, and V. M. Vinokur, Rev. Mod. Phys. **66**, 1125 (1994).

[2] D. Nelson and V. M. Vinokur, Phys. Rev. B **48**, 13 060 (1993).

[3] T. Hwa, D. Nelson, and V. M. Vinokur, Phys. Rev. B **48**, 1167 (1993).

[4] L. Civale *et al.*, Phys. Rev. Lett. **67**, 648 (1991).

[5] W. K. Kwok *et al.*, Phys. Rev. Lett. **69**, 3370 (1992).

[6] H. K. Olsson *et al.*, Phys. Rev. Lett. **66**, 2661 (1991).

[7] Hui Wu, N. P. Ong, and Y. Q. Li, Phys, Rev. Lett. **71**, 2642 (1994).

[8] D. G. Xenikos *et al.*, Physica C **235-240**, 2661 (1994).

[9] M. Golosovski *et al.*, Phys. Rev. B **50**, 470 (1994).

[10] S. Revenaz *et al.*, Phys. Rev. B **50**, 1178 (1994).

[11] A. E. Koshelev and V. M. Vinokur, Physica C **173**, 465 (1991).

[12] M. V. Feigel'man and V. M. Vinokur, Phys. Rev. B **41**, 8986 (1990).

[13] E. J. Tomlinson, P. Przyslupski, and J. E. Evetts, Cryogenics **33**, 28 (1993).

[14] R. A. Doyle, A. M. Campbell, and R. E. Somekh, Phys. Rev. Lett. **71**, 4241 (1993).

[15] E. R. Ulm *et al.*, Phys. Rev. B **51**, 9193 (1995); S. J. Turneaure, E. R. Ulm, and T. R. Lemberger (unpublished).

[16] D. S. Pyun, E. R. Ulm, and T. R. Lemberger, Phys. Rev. B **39**, 4140 (1989).

[17] M. N. Kunchur, D. K. Christen, and J. M. Phillips, Phys. Rev. Lett. **70**, 998 (1993).

[18] J. R. Clem and M. W. Coffey, Phys. Rev. B **50**, 470 (1994).

[19] Extensive experimental work has been published on the subject, including that in Refs. 6–8. General scaling arguments can relate the value of the exponent ζ at the glass transition T_g to the dynamical critical exponent z of the transition [e.g., $\zeta = 1/z$ in the framework of the vortex-glass model and $\zeta = 3/(2z-1)$ in the Bose glass]. Furthermore, numerical simulations of R. Sasik and D. Stroud [Phys. Rev. Lett. **73**, 2662 (1994)] for YBCO have shown the existence of a melting transition where L_V diverges as $f \rightarrow 0$.

[20] R. H. Koch *et al.*, Phys. Rev. Lett. **63**, 1511 (1989).

[21] D. G. Xenikos, J.-T. Kim, and T. R. Lemberger, Phys. Rev. B **48**, 7742 (1993); D. G. Xenikos and T. R. Lemberger, Physica B **194-196**, 1913 (1994).